

Long Baseline Hardware Gradiometer Based on HTS rf-SQUIDs With Substrate Resonators

Grigory I. Panaitov, Yi Zhang, Hans-Joachim Krause, Jürgen Schubert, and Marko Banzet

Abstract—We have developed an asymmetric thin film first order gradiometer based on an HTS rf-SQUID. A coupling scheme uses an SrTiO_3 substrate resonator as an rf-tank circuit which simplifies the gradiometer balancing. Advantage of the technique is that gradiometers with very long baseline can be fabricated. The performance of 13 mm and 33 mm baseline SQUID gradiometers is presented. The gradiometers have been successfully used in applications for nondestructive evaluation of materials.

Index Terms—Gradiometer, magnetic sensor, SQUID.

I. INTRODUCTION

IN many applications the background environmental noise is a few orders of magnitude higher than the intrinsic noise of superconducting interference devices (SQUIDs). To reduce the external noise and realize the highest sensitivity of SQUIDs a magnetic shielding is usually used in measurements. An alternative approach is to use a SQUID gradiometer which suppresses the common mode of the background signal [1]. Due to the lack of high-quality high temperature superconducting (HTS) wires, HTS SQUID gradiometers are usually operated in the configuration of an electronic gradiometer [2]. However, a hardware gradiometer has the advantage that it can be operated in presence of external noise with an amplitude exceeding the dynamic range of the SQUID magnetometer. Many attempts have been made to develop HTS thin film planar gradiometers based on dc- and rf-SQUIDs [3]–[6]. The main problem of dc-SQUID based gradiometers is that the dc-SQUID itself has a nonzero response to magnetic field which reduces the gradiometer balance. In an rf-SQUID of so-called, 'two hole' Zimmerman type structure, [7], this problem is eliminated but the maximum gradiometer baseline is limited to about 5 mm due to large inductance of the device loop [8]. A quite different approach to single layer planar gradiometer was demonstrated recently by Dantsker *et al.* [9]. A dc-SQUID was coupled inductively to an asymmetric flux transformer in flip-chip configuration. At some suitable inductive coupling between SQUID and transformer this arrangement can operate as a first order planar gradiometer. Based on this technique gradiometers with very large baseline can be fabricated. With an appropriate transformer configuration, this arrangement can be extended to even higher order planar gradiometers [10].

Manuscript received August 5, 2002. This work was supported in part by German BMBF under Grant 13N7739/9.

The authors are with the Institute of Thin Films and Interfaces, Research Center Jülich GmbH, 52425 Jülich, Germany (e-mail: g.panaitov@fz-juelich.de).

Digital Object Identifier 10.1109/TASC.2003.814063

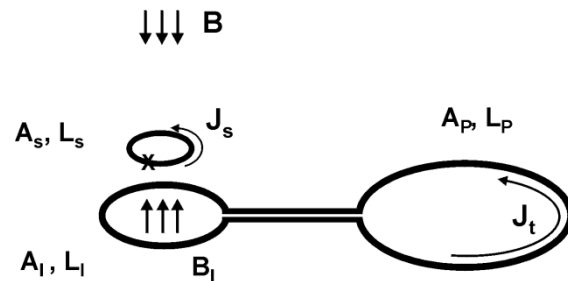


Fig. 1. Schematic of the planar SQUID gradiometer with an asymmetric flux transformer. The SQUID is inductively coupled to the input coil of the transformer. Arrows near pick-up loop and SQUID indicate the screening currents due to applied field (B). A and L denote area and inductance of SQUID, input and pick-up coils.

We have developed a first order planar gradiometer based on a HTS rf-SQUID with a substrate resonator as the rf-tank circuit. The technique which we have used simplifies the balancing procedure of the gradiometer.

II. EXPERIMENTAL

A. Principle and Schematic of the Gradiometer

The idea of the SQUID gradiometer with the asymmetric flux transformer is schematically illustrated in Fig. 1. The SQUID is inductively coupled to a superconducting flux transformer consisting of pickup coil and input coils (A and L denote area and inductance of the loops). Basically, the presented setup looks exactly the same as the setup of a typical SQUID magnetometer with a flux transformer. The principal difference is that in a magnetometer the SQUID and the input coil are placed in a magnetic shield, and only the pick-up coil is exposed to the measuring magnetic field B . To operate this setup as a gradiometer both, pick-up and input coil coupled to SQUID have to be in the magnetic field. One more requirement is needed, the pick-up coil have to be larger than the input coil, ($A_p \gg A_i$). In this case, the pick-up coil delivers a large screening current which creates a magnetic field, B_i , with the amplitude larger than the applied field, $|B_i| > |B|$, and oppositely directed. In the gradiometer SQUID is positioned, so that from one side it is exposed to the applied field B and from other side it is coupled to the oppositely directed field of the input coil B_i . If the coupling to both fields is equal then the gradiometer is balanced. This is the simplified picture of the physics behind a gradiometer with an asymmetric flux transformer. Following Dantsker *et al.* [9], we can calculate exactly the coupling coefficient which is needed to balance the gradiometer. From expressions for the flux conservation in the

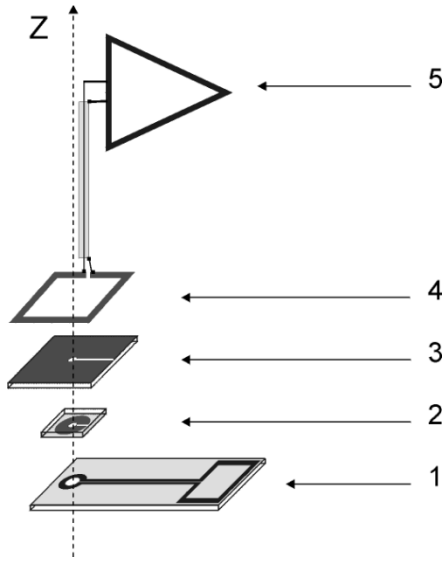


Fig. 2. Arrangement of the gradiometer with rf-SQUID and an asymmetric flux transformer. The flux transformer (1) and SQUID (2) are inductively coupled in flip-chip configuration. A substrate of SrTiO_3 (3) is used as a resonant tank circuit. The whole package connected to readout electronics (5) via a coupling loop (4).

transformer and in the SQUID loop we find the screening super-current in the SQUID if the gradiometer is exposed to a uniform magnetic field B_z :

$$J_s = \frac{B_z \left[\frac{M(A_i + A_p)}{(L_i + L_p)} - A_s \right]}{\left[\frac{M^2}{(L_i + L_p)} - L_s \right]} \quad (1)$$

where $M = k\sqrt{L_i L_s}$ – the mutual inductance between SQUID and input coil. We assume that the inductance of the striplines is negligible. If we take the coupling coefficient:

$$k = \frac{[A_s(L_i + L_p)]}{[\sqrt{L_i L_s}(A_i + A_p)]} \quad (2)$$

then the current (1) in SQUID loop is $J_s = 0$, i.e., the sensor becomes insensitive to a uniform field. If the applied field has a nonzero gradient component $\delta B_z / \delta x$ the current in the SQUID is:

$$J_s = \left[\frac{MA_p l}{(M^2 + L_s(L_i + L_p))} \right] \frac{\delta B_z}{\delta x} \quad (3)$$

where l is the baseline. So, the sensor output is proportional to the field gradient, i.e., it operates as a first order gradiometer.

B. Gradiometer Arrangement

The arrangement of the gradiometer we have designed is schematically shown in the Fig. 2. Two types of flux transformers have been fabricated from YBCO thin films deposited on the LaAlO_3 substrates $10 \text{ mm} \times 20 \text{ mm}$ and $10 \text{ mm} \times 40 \text{ mm}$. The geometrical baseline of the gradiometer structures were 13 mm and 33 mm. The size of pick-up and input coils is chosen to satisfy the restrictions of expression (2). The gradiometer can be balanced only if the calculation of the coupling coefficient by (2) yields: $k < 1$. This requirement leads basically to $A_p > A_i$ and $L_p > L_i$. A 3.5 mm washer

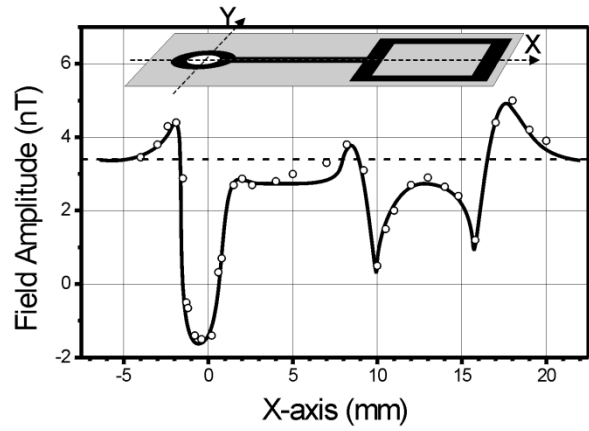


Fig. 3. Field distribution along the x -axis of the flux transformer exposed to a uniform magnetic field 3.4 nT. Circles are the measured data while thick line is a spline approximation. The inset on the top shows schematically the transformer and axes of coordinate system.

rf-SQUID was inductively coupled to the flux transformer in flip-chip configuration. As rf-tank circuit, we used a SrTiO_3 substrate resonator, which resonates at about 600 MHz. Details of the rf-SQUID with substrate resonator we have used, can be found in [11]. The inductive coupling between SQUID and flux transformer was changed by a fine mechanical variation of the distance between two substrates. In order to simplify the balancing procedure, we have investigated first the field distribution around of the flux transformer exposed to a uniform magnetic field.

C. Field Profiles

A homogeneous magnetic field 3.4 nT at 13 Hz was applied to the flux transformer in the z -direction, i.e., perpendicular to the substrate surface. The field around the flux transformer was measured with a SQUID sensor using the lock-in technique. An example of the field profile along x -axis of the flux transformer with baseline 13 mm is presented in Fig. 3. The inset on the top of the figure shows the geometry of the experiment. Both x - and y -axes lie on the substrate surface while z -one is directed normally to the substrate. The circles on the figure are the data taken at $z = 0.2$ and $y = 0.5$ mm. The dashed line indicates the level of the applied field, whereas the thick line is a spline approximation. The measured field profile agrees qualitatively with the field distribution expected from the transformer current. The most important is that the profile line crosses the zero field level and the field inside of the input loop is negative. There are two 'zero points,' or crossover points, at about $x = 0.8$ mm and $x = -1.2$ mm, where the signal response is zero. Actually, these are, so-called, balance points i.e., exactly at these x -distances between transformer and SQUID the system is insensitive to a uniform field, thus it works as balanced gradiometer. By variation of the x -distance we drove the gradiometer to balanced condition. The difficulty of this procedure is that the variation of the field round of balance points is very strong. That is why the balance technique requires a very fine mechanics to adjust the coupling between SQUID and input coil to an optimum. Fig. 4 shows that even a very small variation of the relative x -distance between SQUID and input coil in vicinity of the maximum leads

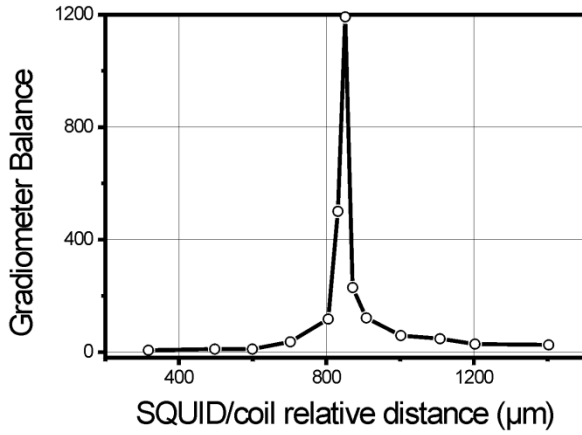


Fig. 4. Balance coefficient of the gradiometer with the asymmetric flux transformer as a function of the relative distance between SQUID and input coil.

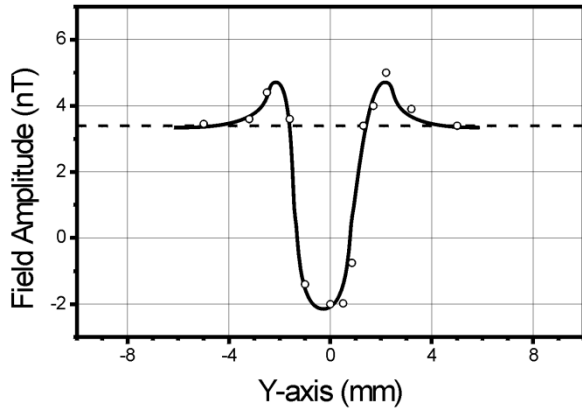


Fig. 5. Field distribution across the input coil of the flux transformer in y -direction. Circles are the measured data while thick line is a spline approximation. The field profile has been measured in a uniform magnetic field 3.4 nT (dashed line).

to the drop of the balance parameter down to a few orders of magnitude. In this case, the balance parameter was calculated as the ratio between output signals of balanced and completely nonbalanced gradiometer. The latter was measured with the balanced gradiometer the pick-up coil of which was covered by a superconducting film.

Of course the two crossover points in the Fig. 3 are not the only balance points in the designed gradiometer. Trying to find the better adjustment procedure, we have investigated also the field profiles round of the input coil along the y - and z -axes. Fig. 5 shows the y -profile of the field distribution across the input coil at $x = 0$. The y -field profile contains another two balance points, at about $y = 1$ mm and $y = -1$ mm, where the profile curve crosses the zero-field level. The field gradient $\delta B/\delta y$ at these balance points is still high. In this sense, the balance procedure by variation of the y -distance has no advantages compared to x -adjustment. The gradiometer can be balanced also by changing the z -distance between SQUID and flux transformer substrates. Fig. 6 shows the field distribution along the z -symmetry axis of the input coil. The data (circles) are taken at $x = 0$, $y = 0$. The measurement is in a good agreement with the field profile of the circular current in the input coil (thick line) calculated by: $B_z \sim \mu_0 I/z^3$. The field dependence in the

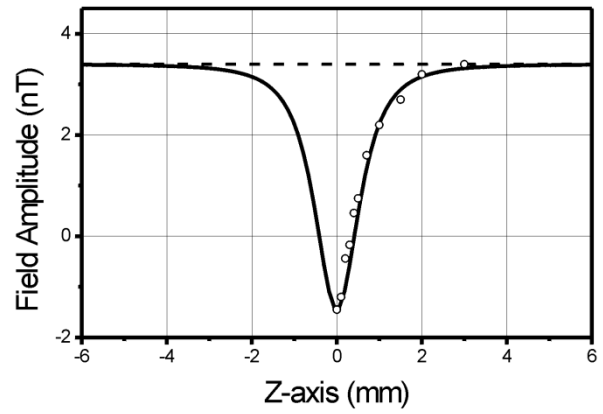


Fig. 6. Field distribution along the z -axis of the input coil. Circles are the measured data while the thick line is the calculation of the axial field. The data have been taken at a uniform magnetic field 3.4 nT (dashed line).

Fig. 6 has another crossover point at about $z = 0.5$ mm, which also can be used to balance the gradiometer.

D. Balance of the Gradiometer

The analysis of field profiles shows that for the input coil of a circular geometry all balance points are situated on the surface of a 3-D elliptical sphere with the symmetry axis lying on the z -axis. It is obvious, that field derivatives $\delta B/\delta x$ and $\delta B/\delta y$ have a minimum on the top of this sphere, at $x = 0$, $y = 0$ and $z = 0.5$ mm in our case. The region $z \leq 0.5$ mm is more suitable for the controllable adjustment of the gradiometer to the optimum balance condition.

In order to control the z -distance between SQUID and flux transformer substrates we have used Mylar foils of different thickness. The reproducible balance coefficients of about 1500 and 1200 could be obtained for gradiometers with baseline 13 mm and 33 mm, respectively. We could get better balance parameters but the reproducibility of highly balanced gradiometers with the adjustment mechanics we have used still remained problematic. Another problem which limited the balance performance are the mechanical imperfections, e.g., due to the small misalignment of the SQUID and transformer substrates. The nonuniformity of the calibrating homogeneous field was another important option by balance of the gradiometer with the long baseline. In general, the output of the gradiometer is:

$$V_g = G \left[b^{-1} B_z + \left(\frac{\delta B_z}{\delta x} \right) l \right] \quad (4)$$

where G is the gain, b – balance coefficient, which determines the rejection of the common mode field B_z , and l is the baseline. Here, we neglected the eddy current component in the output of the gradiometer which is important at high frequency ac-field [1]. Equation (4) shows, that the longer baseline the larger the gradient component, i.e., the larger balance error due to non-homogeneity of the calibrating field. For the gradiometer with baseline $l = 33$ mm this factor is about one order higher than for thin film gradiometers prepared on the substrate $10 \text{ mm} \times 10 \text{ mm}$. In our experiments the calibrating homogeneous field has been created by a Helmholtz coil system of $2 \text{ m} \times 2 \text{ m} \times 2 \text{ m}$ size. The effective area of the gradiometer, $\delta \Phi/\delta B$, has been

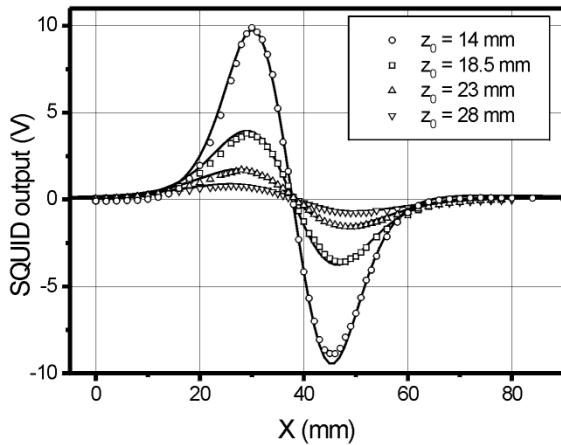


Fig. 7. Signal of the z -magnetic dipole as a function of scanning distance x . Symbols are the data measured at, z_0 , distances between the dipole and the gradiometer which are noted in the figure inset. Thick lines are calculations of the expected gradiometer output for baseline $l = 13.5$ mm.

determined to be about 0.2 mm^2 . In order to determine the effective baseline, we have analyzed the signal of a magnetic dipole measured with the gradiometer. The z -dipole has been moved under the gradiometer in x -direction and z -component of the field has been taken at different distances between the dipole and gradiometer, z_0 . Fig. 7 shows the result of the measurement. Symbols in the Fig. 7 are the measured data while thick lines are the gradient signals which we have calculated using the (5):

$$\frac{\delta B_z}{\delta x} = \frac{\mu_0 M}{4\pi l} \left[\frac{2z_0^2 - x^2}{x^2 + z_0^2} - \frac{2z_0^2 - (x-l)^2}{(x-l)^2 + z_0^2} \right] \quad (5)$$

where \mathbf{M} is the magnetic moment of the dipole, \mathbf{l} is the baseline. The (5) we have derived using the well known formulae of the field of a localized magnetic dipole. Four distances z_0 are taken, as used in the measurement: $z_0 = 14$ mm, 18.5 mm, 23 mm and 28 mm. The fit to the measured data yields an effective baseline of about 13.5 mm, which agrees very well with the geometrical baseline 13 mm. This is the indication of the well defined gra-

diometer structure with negligible effective area of the striplines between the input and pick-up coils. The white noise of the unshielded gradiometer has been about $100 \text{ fT}/\sqrt{\text{Hz}}$, which is worse than we expected using the SQUIDS with white noise of about $40 \text{ fT}/\sqrt{\text{Hz}}$. In order to improve the noise performance we have to optimize the coupling between the rf-resonator and SQUID. However, the quality of the designed is good enough for applications in nondestructive evaluation technique.

REFERENCES

- [1] J. Vrba, "SQUID gradiometers in real environment," in *SQUID Sensors: Fundamentals, Fabrication and Applications*, H. Weinstock, Ed. Dordrecht: Kluwer Academic Pbl., 1996, pp. 63–116.
- [2] Y. Tavrín, Y. Zhang, W. Wolf, and A. I. Braginski, "A second order SQUID gradiometer operating at 77 K," *Supercond. Sci. Technol.*, vol. 7, pp. 265–268, 1994.
- [3] M. B. Ketchen, W. M. Goubau, J. Clarke, and G. B. Donaldson, "Superconducting thin film gradiometer," *J. Appl. Phys.*, vol. 49, pp. 4111–4116, 1998.
- [4] S. Wunderlich, F. Schmidl, H. Sprecht, L. Dörrer, H. Schneidewind, U. Hübner, and P. Seidel, "Planar gradiometers with high- T_c SQUIDS for nondestructive testing," *Supercond. Sci. Technol.*, vol. 11, pp. 315–321, 1998.
- [5] Y. Zhang, H. Soltner, H.-J. Krause, E. Sodtke, W. Zander, J. Schubert, M. Grünekle, D. Lomparski, M. Banzet, H. Bousack, and A. Braginski, "Planar HTS gradiometer with large baseline," *IEEE Trans. Appl. Supercond.*, vol. 7, pp. 2866–2869, 1997.
- [6] V. Zakosarenko, K.-H. Berthel, K. Blütner, P. Seidel, and P. Weber, "Thin film dc SQUID gradiometer using using a single YBCO layer," *Appl. Phys. Lett.*, vol. 65, pp. 779–780, 1994.
- [7] J. E. Zimmerman, P. Thiene, and J. T. Harding, *J. Appl. Phys.*, vol. 41, p. 1572, 1970.
- [8] M. Maus, M. Vaupel, H.-J. Krause, Y. Zhang, H. Bousack, R. Kutzner, and R. Wördenweber, "HTS RF SQUID planar gradiometer with long baseline for the inspection of aircraft wheels," in *Applied Supercond. (1999)*, *Proc. of EUCAS'99*, vol. 2, 2000, pp. S.457–460.
- [9] E. Dantsker, O. Froehlich, S. Tanaka, K. Kousnetsov, J. Clarke, Z. Lu, V. Matijasevic, and K. Char, "High- T_c superconducting gradiometer with a long baseline asymmetric flux transformer," *Appl. Phys. Lett.*, vol. 71, pp. 1712–1714, 1997.
- [10] A. Kittel, K. A. Kouznetsov, R. McDermott, B. Oh, and J. Clarke, "High- T_c superconducting second-order gradiometer," *Appl. Phys. Lett.*, vol. 73, pp. 2197–2199, 1998.
- [11] Y. Zhang, J. Schubert, N. Wolters, M. Banzet, W. Zander, and H.-J. Krause, "Substrate resonator for HTS rf SQUID operation," *Physica C*, 2002, to be published.